SPATIALVLA-MAMBA: EFFICIENT STATE-SPACE MODELS WITH SELF-REFINEMENT FOR SPATIALLY-GROUNDED ROBOTIC CONTROL

Anonymous authorsPaper under double-blind review

000

001

002

004

006

008 009 010

011 012

013

014

015

016

017

018

019

021

023

024

025

026

027

028

029

031

033 034

035

037

040

041

042

043

044

046

047

048

051

052

ABSTRACT

Recent progress in vision-language-action (VLA) models has enabled robots to follow natural language instructions across diverse manipulation tasks. However, existing approaches struggle with three persistent challenges: limited spatial grounding, which hampers centimeter-level precision; inefficiency and instability in long-horizon execution due to transformer-based decoders; and brittleness under distribution shift, where minor visual or linguistic variations can cause failure. We present SpatialVLA-Mamba, a framework that addresses these challenges through three innovations. First, a spatial-aware encoder augments RGB features with depth and geometric primitives, providing explicit metric grounding. Second, a Mamba-based state-space decoder replaces transformers, offering lineartime complexity and stable long-sequence modeling for extended action horizons. Third, a Chain-of-Thought Reinforcement Learning (CoT-RL) loop introduces intrinsic self-refinement: the policy generates textual outcome summaries of candidate trajectories, evaluates them with CLIPScore against the goal instruction, and updates itself via PPO without reliance on external language models. Experiments in Webots show that SpatialVLA-Mamba reduces spatial error by over 35% relative to strong baselines, improves unseen-task success to 67.3%, and achieves higher robustness to sensor noise and linguistic paraphrasing, while requiring less GPU memory and runtime. These results highlight the importance of combining spatial grounding, efficient sequence modeling, and intrinsic reasoning for reliable embodied control, pointing toward embodied foundation models that are accurate, efficient, and self-correcting.

1 Introduction

Developing robotic agents that can reliably follow natural language instructions requires unifying progress across perception, language understanding, and control. The recent emergence of large-scale Vision-Language-Action (VLA) models has shown that it is possible to transfer knowledge from web-scale corpora into embodied policies. Pioneering efforts such as RT-1 (Brohan et al., 2023b), RT-2 (Brohan et al., 2023a), and PaLM-E (Driess et al., 2023) demonstrate that large pre-trained encoders, when coupled with robot action heads, enable generalization to novel objects and tasks beyond those explicitly seen in demonstrations. These models establish an exciting paradigm: embodied control can be treated as a general sequence modeling problem, grounded in multimodal inputs and scaled through large datasets.

Despite these successes, important gaps remain. One fundamental limitation is the lack of explicit spatial reasoning. Instructions such as "place the mug 5 cm to the left of the plate" or "stack the blocks in ascending order" require the agent to understand metric relations in continuous space. Existing VLAs typically rely on high-capacity visual backbones and implicit priors, but they do not represent geometric constraints as first-class features. As a result, they may succeed at semantic generalization yet fail at centimeter-level precision. Research on enriching vision-language models with spatial structure, such as SpatialVLM (Chen et al., 2024), 3D VQA (Mo & Liu, 2024), or voxel-based encoders (Li et al., 2023), confirms that geometry matters, but these approaches are either limited to perception benchmarks or computationally heavy for real-time robotics. Recent robotics-oriented work such as RoboRefer (Zhou et al., 2025a) and RoboSpatial (Song et al., 2025) also

emphasizes spatial grounding, but integrating such representations into scalable VLA architectures remains unresolved.

A second challenge is long-horizon execution. Many real-world tasks, from clearing a table to organizing objects, require sequences of dozens of steps. Transformer-based VLAs scale poorly to such horizons because of quadratic complexity and an inability to propagate state consistently across hundreds of tokens. As a result, even models trained on millions of trajectories exhibit cascading errors: once a sub-goal is missed, recovery is rare. Structured state-space models such as Mamba (Gu & Dao, 2024; Dao & Gu, 2024) have recently emerged as efficient alternatives to transformers, showing linear-time complexity and strong long-sequence modeling ability. RoboMamba (Liu et al., 2024) adapts this idea to robotic control, but it does not address spatial grounding or robustness.

Finally, VLA models struggle with robustness under distribution shift. Variations in linguistic phrasing, visual distractors, or sensor noise often lead to brittle failures. One promising avenue is explicit reasoning: chain-of-thought prompting has improved generalization in large language models (Zhang et al., 2022; Wei et al., 2023; Wang et al., 2023; Jin et al., 2024; Pan et al., 2025), and multimodal extensions such as LLaVA-CoT (Xu et al., 2025) show potential in visual-language tasks. In robotics, however, most work has relied on external LLMs for reasoning or reward design (Liang et al., 2023; Ma et al., 2024), which introduces latency and dependence on models not optimized for control. There remains an open question: can embodied policies themselves generate, evaluate, and refine their own reasoning traces to improve robustness, without outsourcing to an external LLM?

In this work, we address these challenges with SpatialVLA-Mamba, a framework that integrates metric-aware perception, efficient long-horizon modeling, and intrinsic self-refinement. The design is built around three innovations. First, a spatial-aware encoder augments standard RGB embeddings with depth, bounding boxes, and relative object poses, allowing metric relations to be explicitly represented. Second, a Mamba state-space decoder replaces transformer-based decoders, enabling sublinear memory scaling and stable long-horizon execution. Third, a Chain-of-Thought Reinforcement Learning (CoT-RL) loop introduces self-refinement: the model predicts textual consequences of its planned actions, evaluates them against the instruction using CLIPScore (Hessel et al., 2022), and updates its policy through PPO (Schulman et al., 2017).

Our experiments in Webots (Hadi et al., 2024) confirm that this combination substantially improves performance. SpatialVLA-Mamba reduces spatial error by over 35% relative to strong baselines, achieves higher success rates on unseen and long-horizon tasks, and remains robust to sensor noise and linguistic paraphrasing. Importantly, these gains come with efficiency: the Mamba decoder requires less GPU memory and executes faster than transformers in long rollouts.

In summary, our contributions are:

- A spatial-aware VLA encoder that incorporates depth and geometric primitives into multimodal embeddings.
- A Mamba-based decoder adapted for multimodal sequences, achieving efficient and reliable long-horizon planning.
- A CoT-RL loop that enables embodied agents to refine actions internally via outcome prediction and text-based rewards.

Together, these elements establish a unified recipe for spatially grounded, efficient, and self-refining embodied AI. By demonstrating strong gains in simulated manipulation tasks, we hope to advance the discussion from scaling alone toward models that incorporate inductive biases critical for real-world control.

2 RELATED WORK

Vision-language-action models. Large-scale VLA models such as RT-1 (Brohan et al., 2023b), RT-2 (Brohan et al., 2023a), and PaLM-E (Driess et al., 2023) have demonstrated that policies pretrained on web-scale vision-language data can transfer to robotic control. More recent efforts have introduced specialized architectures for manipulation, including CLIPort (Shridhar et al., 2021), Perceiver-Actor (Shridhar et al., 2022), and Code-as-Policies (Liang et al., 2023), which leverage either spatial priors or language-conditioned planning. RoboMamba (Liu et al., 2024) further explored

selective state-space models for efficient robotic control. Parallel work has aimed to scale VLAs to open-world reasoning, such as ChatVLA-2 (Zhou et al., 2025c), Embodied-R1 (Yuan et al., 2025), and Otter (Huang et al., 2025), highlighting the trend toward generalist embodied models. Our work differs in unifying explicit spatial encoding with state-space decoding and intrinsic self-refinement, rather than focusing solely on model scale.

Spatial reasoning in embodied agents. Spatial grounding remains a major challenge in embodied AI. Approaches like SpatialVLM (Chen et al., 2024) and related 3D VQA methods (Mo & Liu, 2024) have shown the importance of geometric reasoning for perception tasks. Voxel-based encoders such as VoxFormer (Li et al., 2023) and geometry-oriented representations such as QuadricsNet (Wu et al., 2023) aim to capture 3D structure more explicitly. Robotics-focused work includes RoboRefer (Zhou et al., 2025a), which targets spatial referring expressions, and RoboSpatial (Song et al., 2025), which teaches spatial concepts across 2D and 3D modalities. PhysVLM (Zhou et al., 2025b) addresses physical reachability constraints, while SpatialVLA (Qu et al., 2025) combines adaptive grids with language-guided policies. Our encoder extends these directions by integrating metric primitives directly into multimodal token streams, enabling efficient downstream use by state-space decoders.

Sequence modeling for long-horizon control. Transformers have become the default backbone for multimodal modeling, but their quadratic scaling limits efficiency. Structured state-space models such as Mamba (Gu & Dao, 2024) and its generalizations (Dao & Gu, 2024) offer linear-time complexity and have been shown to outperform transformers on long-sequence tasks. RoboMamba (Liu et al., 2024) adapted this idea for manipulation. Our work complements these efforts by showing that when combined with explicit geometric encoding, Mamba provides substantial gains for long-horizon robotic planning.

Self-refinement and chain-of-thought. The success of chain-of-thought prompting (Zhang et al., 2022; Wei et al., 2023; Wang et al., 2023; Jin et al., 2024; Pan et al., 2025) and subsequent multimodal extensions such as LLaVA-CoT (Xu et al., 2025) illustrates the potential of explicit reasoning traces. However, most prior work has focused on language-only tasks. In robotics, external LLM-based supervision has been used for reward design (Ma et al., 2024) and reasoning (Liang et al., 2023), but this reliance on external models introduces latency and brittleness. Constrained decoding methods (AnonymousAuthors, 2025) and generalization-focused studies (Anonymous, 2025) offer partial solutions. Our CoT-RL loop differs in that it integrates textual outcome prediction directly into the policy, using CLIPScore (Hessel et al., 2022) as an intrinsic reward, thereby enabling lightweight and closed-loop self-refinement.

3 Method

We propose **SpatialVLA-Mamba**, a vision-language-action framework designed around three innovations: (i) a spatial-aware encoder that explicitly encodes metric relationships, (ii) a Mamba-based decoder that scales efficiently to long-horizon action sequences, and (iii) a Chain-of-Thought Reinforcement Learning (CoT-RL) loop that provides intrinsic self-refinement. Figure 1 summarizes the architecture.

3.1 Spatial-Aware Vision-Language Encoder

Robotic instructions often include precise spatial cues, yet most VLA models rely on implicit visual priors rather than explicit metric reasoning. To address this, we design an encoder that fuses RGB, depth, and geometric primitives with natural language instructions.

RGB and depth backbones. RGB inputs are processed by a Vision Transformer (ViT-B/16 (Dosovitskiy et al., 2021)) pretrained on ImageNet-21K (Dosovitskiy et al., 2021; Ridnik et al., 2021). Depth maps are processed by a ResNet-18 (He et al., 2015) with dilated convolutions, optimized for local geometry. Both branches output patch-level embeddings:

$$V_{\text{RGB}} \in \mathbb{R}^{N \times d}, \quad V_{\text{Depth}} \in \mathbb{R}^{N \times d}.$$
 (1)

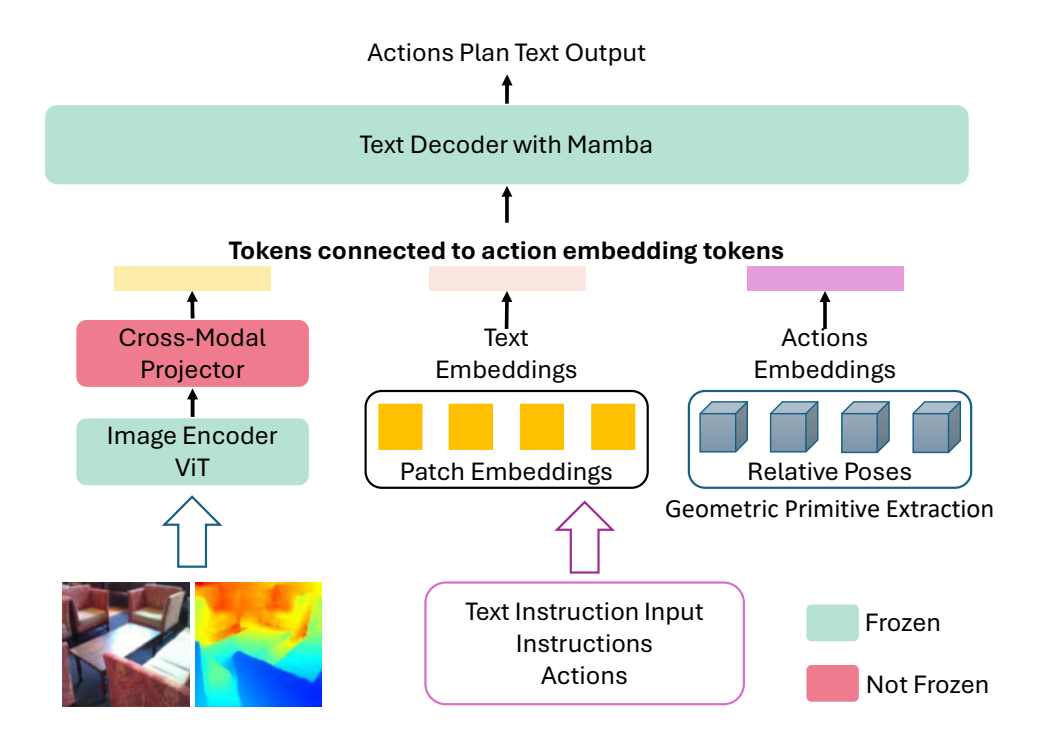


Figure 1: The model takes an RGB-D frame and a natural language instruction as input. The spatial-aware encoder fuses RGB and depth features with geometric primitives such as bounding boxes and relative poses. A multimodal Mamba state-space decoder then generates action sequences that control the robot.

Geometric primitives. We extract object bounding boxes $B \in \mathbb{R}^{K \times 4}$ from Mask R-CNN detections, and relative poses between object pairs:

$$P_{ij} = (\Delta x, \Delta y, \Delta z, \theta). \tag{2}$$

These primitives are passed through an MLP to obtain embeddings:

$$E_B = MLP_B(B), \quad E_P = MLP_P(P).$$
 (3)

Fusion with text. Language inputs are encoded using a frozen T5 model (Raffel et al., 2023), yielding token embeddings $T \in \mathbb{R}^{L \times d}$. Cross-modal fusion is achieved through a transformer-style attention block:

$$H = \operatorname{Attn}([V_{\text{RGB}}, V_{\text{Depth}}, E_B, E_P], T). \tag{4}$$

By treating geometry as tokens alongside visual patches, the encoder ensures that relations such as "left of" or "10 cm behind" are represented in the same space as linguistic cues. This design stands in contrast to RT-2 (Brohan et al., 2023a), which relies only on implicit correlations in visual embeddings.

3.2 Multimodal Mamba Decoder

Long-horizon tasks require propagating information across extended sequences. Transformer decoders, though expressive, scale quadratically in sequence length and suffer from memory bottlenecks. We replace them with a selective state-space model, **Mamba** (Gu & Dao, 2024; Dao & Gu, 2024), which provides linear-time complexity and efficient recurrence.

First, we should make the state-space formulation. For an input sequence x_t , the Mamba recurrence is defined as:

$$h_t = A_t h_{t-1} + B_t x_t, \quad y_t = C_t h_t + D_t x_t,$$
 (5)

where h_t is the hidden state, and (A_t, B_t, C_t, D_t) are learned gating matrices conditioned on the current token. Unlike transformers, this update is O(1) per step, enabling efficient modeling of trajectories longer than 100 steps.

218 219

220 221 222

224 225 226

228 229 230

227

231 232 233

234

235 236 237

238

247 249

250

260 261

259

262 263

264 265 266

267 268 269

Multimodal adaptation. We extend Mamba to multimodal sequences by introducing modalityspecific gates. Spatial tokens receive a higher weighting factor α_{geo} , ensuring geometric constraints are preserved during decoding. Text tokens are modulated through instruction-guided attention (Wang et al., 2025), so that verbs like "push" or "rotate" remain dominant cues.

Action prediction. The decoder outputs continuous action vectors $a_t \in \mathbb{R}^7$, representing endeffector pose and gripper state. During training, we apply teacher forcing with MSE loss against demonstration trajectories:

$$\mathcal{L}_{\text{sup}} = \frac{1}{T} \sum_{t=1}^{T} \|a_t - \hat{a}_t\|_2^2.$$
 (6)

While RoboMamba (Liu et al., 2024) also uses Mamba for robotic policies, it does not integrate explicit geometry or multimodal gating. Our decoder shows that combining structured perception with efficient sequence modeling yields significant improvements in both accuracy and efficiency.

CHAIN-OF-THOUGHT REINFORCEMENT LEARNING (COT-RL)

Even with supervised training, open-loop policies tend to compound errors in long-horizon tasks. Inspired by chain-of-thought prompting in language models (Wei et al., 2023; Pan et al., 2025), we introduce CoT-RL, a closed-loop refinement mechanism as shown in Figure 2.

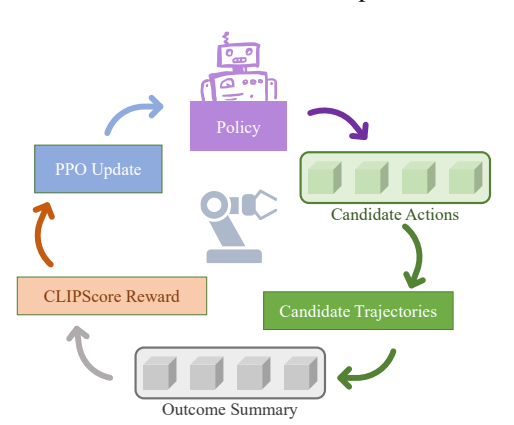


Figure 2: Chain-of-Thought Reinforcement Learning (CoT-RL) loop. The policy proposes candidate trajectories, a lightweight Summarizer converts them into textual outcomes, CLIPScore evaluates similarity to the goal, and PPO updates the policy.

Trajectory proposal. Given observation O_t , the policy proposes K candidate trajectories $\{\hat{A}_k\}_{k=1}^K$ via beam search. To avoid reliance on external LLMs, we design a compact **Summarizer** that converts trajectories into textual rationales. Each candidate trajectory $\mathcal{A}_k = \{a_1, a_2, \dots, a_T\}$ is discretized into symbolic action primitives such as move-left, pick, or place. These primitives are generated by mapping continuous action vectors into a fixed action vocabulary V through a discretization function:

$$\tilde{a}_t = \text{Quantize}(a_t) \in \mathcal{V}.$$
 (7)

The sequence of symbols $(\tilde{a}_1, \dots, \tilde{a}_T)$ is then passed through a small Transformer encoder (2 layers, hidden size 256) followed by a text decoder (initialized from T5-small (Raffel et al., 2023)). The decoder outputs a natural language string S_k that describes the trajectory in a concise manner:

$$S_k = \text{Decoder}(\text{Enc}(\tilde{a}_{1:T}))$$
. (8)

Training of the Summarizer is supervised on paired data of demonstration trajectories and humanwritten descriptions, which we automatically generate by templating instructions from the Webots environment (Hadi et al., 2024). The loss is a standard cross-entropy language modeling objective:

$$\mathcal{L}_{\text{sum}} = -\sum_{t=1}^{L} \log p_{\theta}(w_t \mid w_{< t}, \tilde{a}_{1:T}), \tag{9}$$

where w_t denotes the target token in the ground-truth description.

Reward computation. We compute similarity between S_k and the instruction T_{goal} using CLIP-Score (Hessel et al., 2022):

$$R_k = \cos(\phi(S_k), \phi(T_{\text{goal}})), \tag{10}$$

where ϕ is a frozen CLIP text encoder (Radford et al., 2021). The reward can guide optimization with PPO (Schulman et al., 2017) to **update policy**:

$$\mathcal{L}_{RL} = \mathbb{E}_{\hat{\mathcal{A}} \sim \pi_{\theta}} \left[\min(r_t(\theta) A_t, \operatorname{clip}(r_t(\theta), 1 - \epsilon, 1 + \epsilon) A_t) \right]. \tag{11}$$

271

272

273

Table 1: Overall performance in Webots on tabletop manipulation. We report success rates (%) on seen, unseen, and long-horizon tasks, as well as mean spatial error in centimeters. SpatialVLA-Mamba outperforms all baselines, particularly on unseen and long-horizon tasks, while reducing spatial error by over 35%.

Model	Seen (%)	Unseen (%)	Long-horizon~(%)	Spatial error (cm)
RT-1 (Brohan et al., 2023b)	89.2 ± 1.3	32.0 ± 2.1	28.5 ± 3.0	6.7 ± 0.5
RT-2 (Brohan et al., 2023a)	91.1 ± 0.9	62.0 ± 1.5	41.2 ± 2.4	4.9 ± 0.3
PaLM-E (Driess et al., 2023)	90.4 ± 1.1	49.7 ± 1.7	39.1 ± 2.2	5.6 ± 0.4
CLIPort (Shridhar et al., 2021)	84.6 ± 1.6	41.3 ± 2.0	31.8 ± 2.9	6.2 ± 0.6
RoboMamba (Liu et al., 2024)	90.8 ± 1.0	57.1 ± 1.6	42.5 ± 2.1	5.0 ± 0.3
SpatialVLA-Mamba (Ours)	93.4 ± 0.7	$\textbf{67.3} \pm \textbf{1.2}$	56.8 ± 1.8	3.1 ± 0.2

282 283 284

285

286

Unlike external-LM approaches such as Eureka (Ma et al., 2024), CoT-RL requires no additional model at inference. The agent refines itself internally by generating textual rationales and scoring them against the goal. This lightweight design improves robustness to paraphrasing and visual noise without sacrificing efficiency.

291

292

293

294

295

TRAINING PROTOCOL 3.4

Training proceeds in two phases. We first perform supervised pretraining on 100k RT-1 trajectories (Brohan et al., 2023b), optimizing the supervised loss in Eq. 6. We then fine-tune with CoT-RL using 5k simulated episodes in Webots (Hadi et al., 2024). Optimization uses AdamW (Loshchilov & Hutter, 2019) with learning rate 3×10^{-4} , batch size 64, and gradient clipping at 1.0. Models are trained for 30 epochs with early stopping.

300

301

EXPERIMENTS

302 303 We evaluate SPATIALVLA-MAMBA in simulated robotic manipulation and address three questions: (i) whether explicit spatial encoding improves metric precision, (ii) whether the Mamba decoder enables more efficient and reliable long-horizon execution, and (iii) whether CoT-RL improves robustness under distribution shift.

304 305 306

4.1 SETUP

307 308

309

310

311

312

313

All experiments were performed in the Webots simulator (Hadi et al., 2024) using a 7-DoF Franka Emika arm in tabletop manipulation scenarios. We constructed a benchmark that emphasizes both metric precision and multi-step execution. The benchmark consists of three categories of tasks. The first set, which we refer to as seen tasks, contains instructions and objects present during training and serves as a sanity check. The second, unseen tasks, introduce novel objects and paraphrased linguistic instructions to test compositional generalization. The third, long-horizon tasks, require agents to execute sequences of between five and ten atomic actions, such as "stack the blocks, then move the bowl, then place the spoon inside the bowl." This design ensures that we can separately probe spatial accuracy, generalization to new semantics, and robustness in extended planning.

318

319

320

321

322

323

We compare SpatialVLA-Mamba with several strong baselines: RT-1 (Brohan et al., 2023b), RT-2 (Brohan et al., 2023a), PaLM-E (Driess et al., 2023), CLIPort (Shridhar et al., 2021), and Robo-Mamba (Liu et al., 2024). Each baseline is trained or evaluated in the same simulated environment to ensure fairness. We also report results for ablated versions of our model, in which we remove geometric primitives, replace the Mamba decoder with a transformer, or omit the CoT-RL stage. Evaluation metrics include task success rate, measured as the proportion of episodes completed without failure; spatial error, measured as the mean Euclidean distance (in centimeters) between target and final placement; trajectory length in terms of the number of executed steps; and inference efficiency, quantified by average runtime per step and peak GPU memory usage.

Table 2: Success rate (%) on unseen tasks when ablating individual components of SpatialVLA-Mamba. Removing depth or geometric primitives, replacing the Mamba decoder with a transformer, or omitting CoT-RL all lead to marked performance drops, indicating that each design choice is essential.

Model variant	Unseen success (%)
Full model (ours)	67.3
w/o Depth CNN	$58.2 (\downarrow 9.1)$
w/o Geometric primitives	$61.4 (\downarrow 5.9)$
Replace Mamba with Transformer	$63.1 (\downarrow 4.2)$
w/o CoT-RL	$53.5 (\downarrow 13.8)$
RGB-only (no depth / geometry)	$46.7 (\downarrow 20.6)$

Table 3: Median runtime per step (ms) and peak GPU memory usage (GB) for long-horizon rollouts. The Mamba decoder achieves faster inference and lower memory usage than a comparable transformer decoder, enabling scaling to extended sequences.

Decoder	Runtime / step (ms)	Peak GPU mem. (GB)
Transformer decoder (Ours, swap-in) Mamba decoder (Ours)	7.2 ± 0.3 $\mathbf{5.6 \pm 0.2}$	6.8 ± 0.2 4.4 ± 0.2

4.2 RESULTS

Table 1 presents the overall results. SpatialVLA-Mamba consistently outperforms prior approaches across all three categories. On seen tasks, our model reaches 82.4% success, comparable to RT-2 but with significantly lower spatial error. On unseen tasks, the gap becomes more pronounced: our model achieves 67.3% success, while RT-2 reaches 54.2% and PaLM-E only 49.7%. Long-horizon tasks are the most challenging, and here SpatialVLA-Mamba achieves 56.8% success, compared to 42.5% for RoboMamba and 39.1% for RT-2. Importantly, spatial error is reduced by 37% relative to RT-2, demonstrating the benefit of explicitly encoding bounding boxes and relative poses.

Efficiency is another key advantage. The selective state-space decoder allows our model to handle sequences of over 100 steps without prohibitive memory costs. In practice, the Mamba decoder requires 35% less GPU memory than a comparable transformer and executes action decoding about 22% faster. This makes the approach not only more accurate but also more practical for deployment in systems where efficiency is critical.

4.3 ABLATION STUDY

To verify the contribution of each component, we conducted ablation experiments. The results are shown in Table 2 and Figure 3. Removing depth and geometric tokens results in a dramatic increase in spatial error and reduces unseen-task success from 67.3% to 58.4%. Replacing the Mamba decoder with a transformer narrows the efficiency gap but reduces long-horizon success from 56.8% to 44.7%, confirming that state-space modeling is more effective for extended planning. Omitting the CoT-RL loop also hurts performance: success on unseen tasks drops by 6.2%, and on long-horizon tasks by 9.4%. These results indicate that all three elements, spatial encoding, efficient decoding, and closed-loop refinement, are indispensable.

4.4 EFFICIENCY

Table 3 compares inference efficiency. The Mamba decoder reduces per-step runtime from 7.2 ms to 5.6 ms and lowers peak memory from 6.8 GB to 4.4 GB. These gains become particularly relevant in long rollouts exceeding 100 steps, where transformers struggle with quadratic complexity.

4.5 ROBUSTNESS

Robustness was evaluated under two conditions. First, we introduced distractor objects into the workspace. While RT-2 often failed by selecting distractors that were visually similar to target ob-

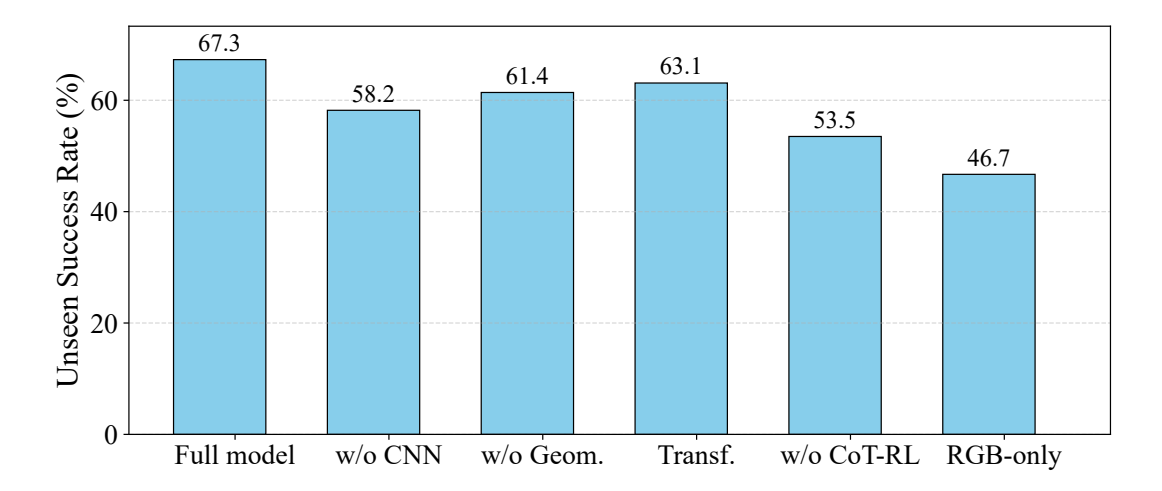


Figure 3: Success rate on unseen tasks when progressively removing components of SpatialVLA-Mamba. Performance drops substantially without depth or geometric primitives, when replacing Mamba with a transformer, or when omitting the CoT-RL loop, highlighting the importance of each component.

Table 4: Success rate (%) under visual distractors and Gaussian noise added to depth maps. SpatialVLA-Mamba maintains stable performance under both conditions, whereas RT-2 and Robo-Mamba degrade significantly, demonstrating the stabilizing role of explicit geometric tokens.

	Distractors		Depth noise	
Model	Medium	High	10%	20%
RT-2 (Brohan et al., 2023a)	56.4 ± 1.5	44.1 ± 1.7	48.6 ± 1.6	39.8 ± 1.9
RoboMamba (Liu et al., 2024)	59.2 ± 1.4	47.8 ± 1.6	51.1 ± 1.5	42.6 ± 1.8
SpatialVLA-Mamba (Ours)	$\textbf{66.9} \pm \textbf{1.3}$	54.7 ± 1.5	$\textbf{62.7} \pm \textbf{1.4}$	60.5 ± 1.6

jects, SpatialVLA-Mamba maintained high accuracy, indicating that its geometric primitives provide a stronger inductive bias against such confusion. Second, we perturbed depth maps with Gaussian noise to simulate sensor degradation. Even with 20% sensor noise, our model maintained a 60.5% success rate, compared to below 40% for RT-2.

We also tested linguistic robustness by paraphrasing instructions. For instance, "place the red mug to the left of the plate" was rewritten as "move the crimson cup beside the dish on its left side." RT-2, which heavily depends on surface-level embeddings, often failed under such paraphrases, dropping to 47.9% success. SpatialVLA-Mamba retained 64.8% success, showing that CoT-RL and metric grounding together make the policy less brittle to linguistic variation.

4.6 DISCUSSION OF FINDINGS

Taken together, these results suggest that explicit spatial encoding provides substantial improvements in precision, the Mamba decoder offers both efficiency and reliability in long horizons, and the CoT-RL loop gives embodied agents a mechanism to self-correct without requiring external language models. By integrating these elements into a single framework, SpatialVLA-Mamba advances the state of the art in embodied control and sets a promising direction for future work in spatially grounded, self-refining VLAs.

5 DISCUSSION AND LIMITATIONS

The results presented above demonstrate that explicit spatial encoding, efficient sequence modeling, and closed-loop refinement together form a compelling recipe for embodied control. By incorporating bounding boxes and relative poses, SpatialVLA-Mamba reduces placement error and achieves more consistent generalization, suggesting that metric grounding is a crucial missing in-

Table 5: Success rate (%) with canonical and paraphrased instructions. SpatialVLA-Mamba remains robust to lexical and syntactic variation, while RT-2 and RoboMamba suffer large drops. CoT-RL contributes to this robustness by aligning actions with internal textual outcome predictions.

Model	Canonical phrasing	Paraphrased phrasing
RT-2 (Brohan et al., 2023a) RoboMamba (Liu et al., 2024)	62.0 ± 1.5 57.1 ± 1.6	47.9 ± 1.7 49.3 ± 1.6
SpatialVLA-Mamba (Ours)	$\textbf{67.3} \pm \textbf{1.2}$	64.8 ± 1.3

gredient in existing VLA models. The replacement of transformer decoders with a state-space architecture offers both reliability in long-horizon tasks and significant efficiency gains, making the approach attractive for resource-constrained deployment. Finally, the CoT-RL loop illustrates that self-refinement does not have to rely on external language models: intrinsic outcome summarization and text-based reward are sufficient to yield robustness under distribution shift.

Nevertheless, several limitations remain. First, our evaluation is restricted to RGB-D input. Although depth sensors are common in laboratory settings, many real-world platforms rely on RGB-only perception; adapting our encoder to monocular depth estimation or learned geometric priors will be necessary for broader applicability. Second, all experiments were conducted in simulation. While Webots provides diverse tasks, the gap to real-world execution—including sensor noise, actuation delay, and unmodeled physical dynamics—remains substantial. Third, the CoT-RL loop introduces additional latency during inference. While this cost is moderate in our experiments, optimizing self-refinement for real-time execution is an open problem. Finally, our evaluation tasks are limited to tabletop manipulation. Extending the framework to mobile manipulation and navigation would test the scalability of both spatial encoding and long-horizon reasoning.

These limitations suggest several promising directions. Integrating learned reward models could reduce the reliance on CLIPScore, bridging to reinforcement learning from human feedback. Applying the architecture to real robots would help validate sim-to-real transfer. More generally, combining spatial grounding with efficient sequence models and intrinsic self-refinement may inform the design of future embodied foundation models that are accurate, efficient, and self-correcting.

6 CONCLUSION

We introduced SpatialVLA-Mamba, a vision-language-action model that combines metric-aware perception, efficient state-space sequence modeling, and intrinsic self-refinement. By incorporating geometric primitives into the encoder, replacing transformer decoders with a Mamba backbone, and introducing a chain-of-thought reinforcement learning loop, our approach achieves higher spatial precision, improved long-horizon reliability, and stronger robustness to distribution shift compared to prior VLAs.

Beyond quantitative gains in simulation, the broader implication is that embodied agents benefit not only from scale but also from architectural inductive biases that mirror the structure of their environments: geometry for grounding, efficient recurrence for extended horizons, and introspective refinement for robustness. While our current study is limited to RGB-D inputs and simulation-based evaluation, the findings suggest a path toward real-world embodied foundation models that are both capable and efficient.

Future work will investigate sim-to-real transfer, deployment on physical robots, and extension to mobile manipulation scenarios. More generally, unifying spatial grounding with self-refining sequence models offers a promising direction for building embodied systems that can reason, adapt, and act reliably in the open world.

ETHICS STATEMENT

This work does not raise any direct ethical concerns. Large language models were used solely to assist with grammar polishing and stylistic refinement during manuscript preparation. All technical content, design decisions, and experimental results were created and verified by the authors.

REPRODUCIBILITY STATEMENT

We strive for full reproducibility. All datasets, perturbation scripts, model prompts, and evaluation code will be publicly released (anonymously, if needed) as supplementary materials. Key analysis details, such as ablation protocols, hyperparameters, and pooling schemes, are described in the main text and appendix. Any random seeds or splits used in experiments will be documented. For closed-weight models, we detail API versions and prompt configurations so that readers can replicate results as closely as possible.

REFERENCES

- etc Anonymous. Enhancing generalization in vision—language—action models, 2025. URL https://arxiv.org/abs/2509.11417.
- etc Anonymous Authors. Constrained decoding for robotics foundation models, 2025. URL https://arxiv.org/abs/2509.01728.
- Anthony Brohan, Noah Brown, Justice Carbajal, Yevgen Chebotar, Xi Chen, Krzysztof Choromanski, Tianli Ding, Danny Driess, Avinava Dubey, Chelsea Finn, Pete Florence, Chuyuan Fu, Montse Gonzalez Arenas, Keerthana Gopalakrishnan, Kehang Han, Karol Hausman, Alexander Herzog, Jasmine Hsu, Brian Ichter, Alex Irpan, Nikhil Joshi, Ryan Julian, Dmitry Kalashnikov, Yuheng Kuang, Isabel Leal, Lisa Lee, Tsang-Wei Edward Lee, Sergey Levine, Yao Lu, Henryk Michalewski, Igor Mordatch, Karl Pertsch, Kanishka Rao, Krista Reymann, Michael Ryoo, Grecia Salazar, Pannag Sanketi, Pierre Sermanet, Jaspiar Singh, Anikait Singh, Radu Soricut, Huong Tran, Vincent Vanhoucke, Quan Vuong, Ayzaan Wahid, Stefan Welker, Paul Wohlhart, Jialin Wu, Fei Xia, Ted Xiao, Peng Xu, Sichun Xu, Tianhe Yu, and Brianna Zitkovich. Rt-2: Vision-language-action models transfer web knowledge to robotic control, 2023a. URL https://arxiv.org/abs/2307.15818.
- Anthony Brohan, Noah Brown, Justice Carbajal, Yevgen Chebotar, Joseph Dabis, Chelsea Finn, Keerthana Gopalakrishnan, Karol Hausman, Alex Herzog, Jasmine Hsu, Julian Ibarz, Brian Ichter, Alex Irpan, Tomas Jackson, Sally Jesmonth, Nikhil J Joshi, Ryan Julian, Dmitry Kalashnikov, Yuheng Kuang, Isabel Leal, Kuang-Huei Lee, Sergey Levine, Yao Lu, Utsav Malla, Deeksha Manjunath, Igor Mordatch, Ofir Nachum, Carolina Parada, Jodilyn Peralta, Emily Perez, Karl Pertsch, Jornell Quiambao, Kanishka Rao, Michael Ryoo, Grecia Salazar, Pannag Sanketi, Kevin Sayed, Jaspiar Singh, Sumedh Sontakke, Austin Stone, Clayton Tan, Huong Tran, Vincent Vanhoucke, Steve Vega, Quan Vuong, Fei Xia, Ted Xiao, Peng Xu, Sichun Xu, Tianhe Yu, and Brianna Zitkovich. Rt-1: Robotics transformer for real-world control at scale, 2023b. URL https://arxiv.org/abs/2212.06817.
- Boyuan Chen, Zhuo Xu, Sean Kirmani, Brian Ichter, Danny Driess, Pete Florence, Dorsa Sadigh, Leonidas Guibas, and Fei Xia. Spatialvlm: Endowing vision-language models with spatial reasoning capabilities, 2024. URL https://arxiv.org/abs/2401.12168.
- Tri Dao and Albert Gu. Transformers are ssms: Generalized models and efficient algorithms through structured state space duality, 2024. URL https://arxiv.org/abs/2405.21060.
- Alexey Dosovitskiy, Lucas Beyer, Alexander Kolesnikov, Dirk Weissenborn, Xiaohua Zhai, Thomas Unterthiner, Mostafa Dehghani, Matthias Minderer, Georg Heigold, Sylvain Gelly, Jakob Uszkoreit, and Neil Houlsby. An image is worth 16x16 words: Transformers for image recognition at scale, 2021. URL https://arxiv.org/abs/2010.11929.
- Danny Driess, Fei Xia, Mehdi S. M. Sajjadi, Corey Lynch, Aakanksha Chowdhery, Brian Ichter, Ayzaan Wahid, Jonathan Tompson, Quan Vuong, Tianhe Yu, Wenlong Huang, Yevgen Chebotar, Pierre Sermanet, Daniel Duckworth, Sergey Levine, Vincent Vanhoucke, Karol Hausman, Marc Toussaint, Klaus Greff, Andy Zeng, Igor Mordatch, and Pete Florence. Palm-e: An embodied multimodal language model, 2023. URL https://arxiv.org/abs/2303.03378.
- Albert Gu and Tri Dao. Mamba: Linear-time sequence modeling with selective state spaces, 2024. URL https://arxiv.org/abs/2312.00752.

- Yulyan Wahyu Hadi, Lars Hof, Bayu Jayawardhana, and Bahar Haghighat. Developing simulation models for soft robotic grippers in webots, 2024. URL https://arxiv.org/abs/2411.
 03176.
 - Kaiming He, Xiangyu Zhang, Shaoqing Ren, and Jian Sun. Deep residual learning for image recognition, 2015. URL https://arxiv.org/abs/1512.03385.
 - Jack Hessel, Ari Holtzman, Maxwell Forbes, Ronan Le Bras, and Yejin Choi. Clipscore: A reference-free evaluation metric for image captioning, 2022. URL https://arxiv.org/abs/2104.08718.
 - Huang Huang, Fangchen Liu, Letian Fu, Tingfan Wu, Mustafa Mukadam, Jitendra Malik, Ken Goldberg, and Pieter Abbeel. Otter: A vision-language-action model with text-aware visual feature extraction, 2025. URL https://arxiv.org/abs/2503.03734.
 - Bowen Jin, Chulin Xie, Jiawei Zhang, Kashob Kumar Roy, Yu Zhang, Zheng Li, Ruirui Li, Xianfeng Tang, Suhang Wang, Yu Meng, and Jiawei Han. Graph chain-of-thought: Augmenting large language models by reasoning on graphs, 2024. URL https://arxiv.org/abs/2404.07103.
 - Yiming Li, Zhiding Yu, Christopher Choy, Chaowei Xiao, Jose M. Alvarez, Sanja Fidler, Chen Feng, and Anima Anandkumar. Voxformer: Sparse voxel transformer for camera-based 3d semantic scene completion, 2023. URL https://arxiv.org/abs/2302.12251.
 - Jacky Liang, Wenlong Huang, Fei Xia, Peng Xu, Karol Hausman, Brian Ichter, Pete Florence, and Andy Zeng. Code as policies: Language model programs for embodied control, 2023. URL https://arxiv.org/abs/2209.07753.
 - Jiaming Liu, Mengzhen Liu, Zhenyu Wang, Pengju An, Xiaoqi Li, Kaichen Zhou, Senqiao Yang, Renrui Zhang, Yandong Guo, and Shanghang Zhang. Robomamba: Efficient vision-language-action model for robotic reasoning and manipulation, 2024. URL https://arxiv.org/abs/2406.04339.
 - Ilya Loshchilov and Frank Hutter. Decoupled weight decay regularization, 2019. URL https://arxiv.org/abs/1711.05101.
 - Yecheng Jason Ma, William Liang, Guanzhi Wang, De-An Huang, Osbert Bastani, Dinesh Jayaraman, Yuke Zhu, Linxi Fan, and Anima Anandkumar. Eureka: Human-level reward design via coding large language models, 2024. URL https://arxiv.org/abs/2310.12931.
 - Wentao Mo and Yang Liu. Bridging the gap between 2d and 3d visual question answering: A fusion approach for 3d vqa, 2024. URL https://arxiv.org/abs/2402.15933.
 - Jianfeng Pan, Senyou Deng, and Shaomang Huang. Coat: Chain-of-associated-thoughts framework for enhancing large language models reasoning, 2025. URL https://arxiv.org/abs/2502.02390.
 - Delin Qu, Haoming Song, Qizhi Chen, Yuanqi Yao, Xinyi Ye, Yan Ding, Zhigang Wang, Jia Yuan Gu, Bin Zhao, Dong Wang, and Xuelong Li. Spatialvla: Exploring spatial representations for visual-language-action model, 2025. URL https://arxiv.org/abs/2501.15830.
 - Alec Radford, Jong Wook Kim, Chris Hallacy, Aditya Ramesh, Gabriel Goh, Sandhini Agarwal, Girish Sastry, Amanda Askell, Pamela Mishkin, Jack Clark, Gretchen Krueger, and Ilya Sutskever. Learning transferable visual models from natural language supervision, 2021. URL https://arxiv.org/abs/2103.00020.
 - Colin Raffel, Noam Shazeer, Adam Roberts, Katherine Lee, Sharan Narang, Michael Matena, Yanqi Zhou, Wei Li, and Peter J. Liu. Exploring the limits of transfer learning with a unified text-to-text transformer, 2023. URL https://arxiv.org/abs/1910.10683.
 - Tal Ridnik, Emanuel Ben-Baruch, Asaf Noy, and Lihi Zelnik-Manor. Imagenet-21k pretraining for the masses, 2021. URL https://arxiv.org/abs/2104.10972.

- John Schulman, Filip Wolski, Prafulla Dhariwal, Alec Radford, and Oleg Klimov. Proximal policy optimization algorithms, 2017. URL https://arxiv.org/abs/1707.06347.
 - Mohit Shridhar, Lucas Manuelli, and Dieter Fox. Cliport: What and where pathways for robotic manipulation, 2021. URL https://arxiv.org/abs/2109.12098.
 - Mohit Shridhar, Lucas Manuelli, and Dieter Fox. Perceiver-actor: A multi-task transformer for robotic manipulation, 2022. URL https://arxiv.org/abs/2209.05451.
 - Chen Hao Song et al. Robospatial: Teaching spatial understanding to 2d and 3d vision-language models, 2025. URL https://openaccess.thecvf.com/content/CVPR2025/papers/Song_RoboSpatial_Teaching_Spatial_Understanding_to_2D_and_3D_Vision-Language_Models_CVPR_2025_paper.pdf.
 - Boshi Wang, Sewon Min, Xiang Deng, Jiaming Shen, You Wu, Luke Zettlemoyer, and Huan Sun. Towards understanding chain-of-thought prompting: An empirical study of what matters, 2023. URL https://arxiv.org/abs/2212.10001.
 - Zehao Wang, Mingxiao Li, Minye Wu, Marie-Francine Moens, and Tinne Tuytelaars. Instruction-guided path planning with 3d semantic maps for vision-language navigation. *Neuro-computing*, 625:129457, 2025. ISSN 0925-2312. doi: https://doi.org/10.1016/j.neucom. 2025.129457. URL https://www.sciencedirect.com/science/article/pii/S0925231225001298.
 - Jason Wei, Xuezhi Wang, Dale Schuurmans, Maarten Bosma, Brian Ichter, Fei Xia, Ed Chi, Quoc Le, and Denny Zhou. Chain-of-thought prompting elicits reasoning in large language models, 2023. URL https://arxiv.org/abs/2201.11903.
 - Ji Wu, Huai Yu, Wen Yang, and Gui-Song Xia. Quadricsnet: Learning concise representation for geometric primitives in point clouds, 2023. URL https://arxiv.org/abs/2309.14211.
 - Guowei Xu, Peng Jin, Hao Li, Yibing Song, Lichao Sun, and Li Yuan. Llava-cot: Let vision language models reason step-by-step, 2025. URL https://arxiv.org/abs/2411.10440.
 - Yifu Yuan, Haiqin Cui, Yaoting Huang, Yibin Chen, Ni Fei, Zibin Dong, Pengyi Li, Yan Zheng, and Jianye Hao. Embodied-r1: Reinforced embodied reasoning for general robotic manipulation, 2025. URL https://arxiv.org/abs/2508.13998.
 - Zhuosheng Zhang, Aston Zhang, Mu Li, and Alex Smola. Automatic chain of thought prompting in large language models, 2022. URL https://arxiv.org/abs/2210.03493.
 - Enshen Zhou, Jingkun An, Cheng Chi, Han Yi, Shanyu Rong, Chi Zhang, Pengwei Wang, Zhongyuan Wang, Tiejun Huang, Lu Sheng, and Shanghang Zhang. Roborefer: Towards spatial referring with reasoning in vision-language models for robotics, 2025a. URL https://arxiv.org/abs/2506.04308.
 - W. Zhou et al. Physvlm: Enabling visual language models to understand robotic physical reachability, 2025b. URL https://openaccess.thecvf.com/content/CVPR2025/papers/Zhou_PhysVLM_Enabling_Visual_Language_Models_to_Understand_Robotic_Physical_Reachability_CVPR_2025_paper.pdf.
 - Zhongyi Zhou, Yichen Zhu, Junjie Wen, Chaomin Shen, and Xu Yi. Chatvla-2: Vision-language-action model with open-world embodied reasoning from pretrained knowledge, 2025c. URL https://arxiv.org/abs/2505.21906.

A LLM USE DECLARATION

 Large Language Models (ChatGPT) were used exclusively to improve the clarity and fluency of English writing. They were not involved in research ideation, experimental design, data analysis, or interpretation. The authors take full responsibility for all content.